

Computer Simulation and Analysis Methodology for the Detection of Nanostructure in Amorphous Polymers and Elucidation of its Effect on Diffusion Phenomena Therein

C. S. Chassapis^{*+}, D. Spyriouni^{*X}, D. N. Theodorou^{*X} and J. H. Petropoulos^{*}

Abstract – Molecular Dynamics trajectories of oxygen-like spherical molecules within a medium close to that of amorphous polyethylene (PE) are analyzed to detect any formation of nanostructure in the medium and to elucidate mechanistic aspects of penetrant motion. The same analysis is also performed in a medium with flexible chains (FPE). To enable this analysis, reduced trajectories (RT), i.e., sets of equidistant positions along the paths of penetrant molecules are constructed with various step lengths, λ . The degree and prevailing direction of local orientation in the chain liquid are quantified through diagonalization of an orientation tensor defined in the vicinity of RT nodes. As in earlier simulation work, an anomalous (subdiffusive) regime is detected. We approach this regime with fractional differential equations, also applicable in the Fickian regime. The fractality of the trajectory of the penetrants and of the free volume is determined. Directional correlations between steps of RT reveal that the penetrant is temporarily confined within elongated “cavities”. In PE and FPE a clear directional correlation is detected between penetrant displacements and the prevalent orientation of the surrounding polymer; the range of this correlation, on both media, indicates that it is closely related to anomalous diffusion. The automation of the analyses has been accomplished with the creation of a software package that contains a simple scripting language.

Index terms — molecular dynamics, amorphous polymers, nanostructure, reduced trajectories, orientation tensor, subdiffusion, random walk, fractional differential equation, fractal, scripting language.

I. INTRODUCTION

Development of the above methodology was motivated by (a) the fact that, in molecular computer simulations of small molecules diffusing in amorphous polymeric media, deviations from ideal (Einstein) diffusion kinetics, characterized by

$$\lim_{t \rightarrow \infty} \langle (\mathbf{r}_A(t) - \mathbf{r}_A(0))^2 \rangle = 6 D_A t \quad (\text{ideal diffusion kinetics}) \quad (1)$$

corresponding to the broken lines of unit slope in the log-log plots of Fig.1, are often found at small t ; and (b) the need to test and quantify the hypothesis that this anomaly may be a manifestation of non-random nanostructure in the amorphous polymer. For this purpose, a model system was set up [1] consisting of short chains of “united-atom” CH_2 groups and terminal CH_3 groups (represented by

^{*} Demokritos National Research Centre, 15310 Aghia Paraskevi, Athens, Greece.

⁺ Algosystems S.A., 206 Sygrou Ave, 17672 Kallithea, Athens, Greece. Email: cschassapis@acm.org

^X National Technical University of Athens, Athens, Greece.

identical interpenetrating spheres B of diameter σ_B) and O_2 diffusing molecules (represented by spheres A of diameter σ_A) [2]. This system was treated as a microcanonical (NVE) ensemble evolving in time, under the molecular force field generated by (i) simple harmonic B-B bond-stretching, and B-B-B bond-bending, potentials (ii) the intrachain hindered-rotation (torsion) potential and (iii) non-bonded B-B, A-A and A-B truncated Lennard-Jones potentials. It was parameterized and packed to the density required to simulate a real amorphous polyethylene- O_2 system [2] and its evolution was followed by molecular dynamics (MD), at intervals of 6 fs, using a velocity Verlet leapfrog algorithm, for times of several ns per run.

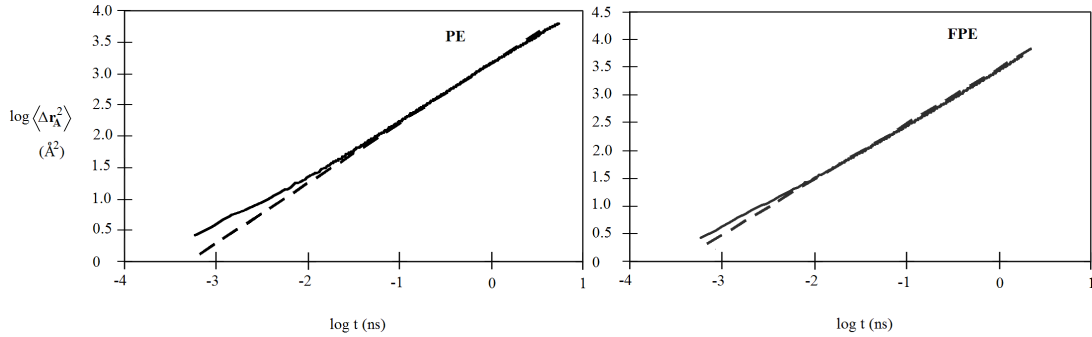


Figure 1. Observed vs. ideal (broken line) diffusion kinetics.

II. MD RESULTS AND ANALYSIS

Analysis of the MD results obtained from the above PE- O_2 model system [1] has yielded material evidence in favor of hypothesis (b). Confirmatory evidence for this hypothesis has now been obtained (see below) from a similar MD study of an FPE- O_2 model system, which was identical with PE- O_2 in all respects, except for the fact that FPE was endowed with much higher chain flexibility by equating its torsional potential to zero.

A. Deviation from Einstein Diffusion – Fractional Equations

As in earlier simulation work, an anomalous (subdiffusive) regime is detected (see Fig. 1), which extends in PE up to times of $\sim 120 - 150$ ps or penetrant displacements of ~ 1.5 nm. In FPE the corresponding values are significantly diminished to $\sim 10 - 50$ ps or ~ 1 nm correspondingly. Anomalous diffusion is the phenomenon where the following behavior is observed [5, 6, 8]

$$\langle \Delta \mathbf{r}_A^2(t) \rangle \sim t^{2/d_w} \quad (2)$$

where the exponent d_w is the anomalous diffusion exponent (also known as the *fractal exponent* of the random walk, is usually non-integer, is equal to $-\log N(\lambda)/\log \lambda$ as $\lambda \rightarrow 0$ and is easily obtainable by log-log plots from our reduced trajectories methodology later described, where $N(\lambda)$ is the number of nodes of the RT of step length λ). Both cases, i.e. super- or sub- diffusion are in general possible, but a random walk in a fractal medium (that we have established is the free volume between the polymeric chains for small time scales, with a fractal exponent $d_f \sim 2.73 - 2.84$, obtained by two methodologies: box counting, and fitting $p(\mathbf{r}_A, t)$ distributions to the solution of the fractional diffusion equation (4) below) is always subdiffusive, i.e. $d_w > 2$, due to the presence of geometric obstacles (the Brownian random walk that is happening during ideal diffusion kinetics, has $d_w = 2$).

The distribution of micromolecules while diffusing is

$$p(\mathbf{r}_A, t) = 4\pi r_A^2 n(\mathbf{r}_A, t) \quad (3)$$

where the prefactor to $n(\mathbf{r}_A, t)$ is the pdf of the distances between uniformly distributed points in space, and $n(\mathbf{r}_A, t)$ is the Van Hove function – the solution to the classical isotropic Diffusion equation. Fitting our $p(\mathbf{r}_A, t)$ data for PE in higher times than 256 ps, gave excellent fits and provided the diffusivities: $D_A = 0.20 - 0.27 \text{ \AA}^2/\text{ps}$ for PE and $D_A = 0.36 - 0.47 \text{ \AA}^2/\text{ps}$ for FPE, that are compatible to the values obtained by applying (1) to Fig 1.

In an effort to understand the non-Fickian regime we made various alterations to the Van Hove function. An imposed time variation of D performed poorly. Exponents in r on the other hand gave excellent results. These findings point to the presence of memory effects in space, and to the presence of singularities in waiting time densities. We tried therefore to understand the subdiffusive regime with fractional differential equations that are also applicable in the Fickian regime.

The anomalous diffusion with correct asymptotic behaviors can be described with the following fractional diffusion equation [8]

$$\frac{\partial^{2/d_w}}{\partial t^{2/d_w}} n(\mathbf{r}_A, t) = D_A \frac{1}{r_A^{d_s-1}} \frac{\partial}{\partial r_A} \left(r_A^{d_s-1} \frac{\partial}{\partial r_A} n(\mathbf{r}_A, t) \right) \quad (4)$$

Comparing this to the classical isotropic diffusion equation in d space dimensions, we see that the Laplacian is altered with the introduction of a non-integer dimension $d_s = 2d_f/d_w$ the spectral or fracton dimension [5,6,8,9], and the time-related differential operator is replaced by a fractional derivative of the order $2/d_w$ defined via a convolution integral. The solution of (4) in the form of a series, was fitted to our $n(\mathbf{r}_A, t)$ data for PE with 3 free parameters: D_A , d_f , d_w and we obtained excellent results for *all* times. By varying the parameters during the fitting we established that the τ_E is near 128 ps. Through this method we also established that: $d_w = 2.10 \pm 0.12$ and $d_f = 2.73 \pm 0.30$.

The theoretical backing of (4) is strong but even this approach is not perfect. The problem is linked to the fact that the polymeric matrix (that creates the free space in which the micromolecules move) moves, and more: it moves subdiffusively ([3], p.10). According to [4], p.124, we must therefore see the $n(\mathbf{r}_A, t)$ of (4) as an average $\langle n(\mathbf{r}_A, t) \rangle$ of the “real” “distribution of distributions” that is multifractal. This discussion gives us a good reason to seek an alternative, simpler, but of enhanced descriptive capacity model of the diffusive behavior in our system for *all* time scales. Our studies show that the fractality of the free volume is lost sooner than the time it takes the random walker to approach the Fickian regime. This allows us proceed as follows: we keep the fractality of time on small time scales and we admit a Euclidean space filled with temporary cages, and we form the equation

$$\left[\left(\tau^\beta \frac{\partial^\beta}{\partial t^\beta} + 1 \right) \frac{\partial}{\partial t} - D_A \nabla^2 \right] n(\mathbf{r}_A, t) = 0 \quad (5)$$

that is a generalized telegrapher’s equation, a “*fractional telegrapher’s equation*” that can describe all time scales accurately (the very short times, the intermediate subdiffusive small times and the Fickian large times). We solve it, accepting that all A molecules are at $r = 0$ for $t = 0$, and the result is

$$\langle \Delta r_A^2(t) \rangle = 2D_A d t \sum_{k=0}^{\infty} \frac{(-1)^k}{\Gamma(2+\beta(k+1))} \left(\frac{t}{\tau} \right)^{\beta(k+1)} \xrightarrow{t \rightarrow \infty} 2D_A d t \left(1 - \frac{1}{\Gamma(1-\beta)} \left(\frac{t}{\tau} \right)^{-\beta} \right) \quad (6)$$

From theoretical calculations using the Rouse model for the chains in our system, studying the liberation of a micromolecule by the chain-made cage, we find that τ should be a few picoseconds.

The important issue is to give physical justification of (5). It can be shown that this justification is reduced to understand the flux for short times when no concentration gradient is present:

$$\tau^\beta \frac{\partial^\beta}{\partial t^\beta} \mathbf{j}(\mathbf{r}_A, t) = 0, \quad \text{for } t \ll \tau \left(\frac{\Gamma(2\beta)}{\Gamma(\beta)} \right)^{1/\beta} \quad (7)$$

with solution:

$$\mathbf{j}(\mathbf{r}_A, t) = \mathbf{J}_0(\mathbf{r}_A) \frac{\tau^{-\beta}}{\Gamma(\beta)} t^{\beta-1} \quad \text{and} \quad n(\mathbf{r}_A, t) = n(\mathbf{r}_A, 0) + \nabla \mathbf{J}_0(\mathbf{r}_A) \frac{1}{\Gamma(1+\beta)} (t/\tau)^\beta \quad (8)$$

Such behaviour can be generated by appropriately confined micromolecules (see Fig. 2). If we assume that each micromolecule, while in captivity, vibrates (mainly parallel to \mathbf{v}_1), then, a distribution of vibration frequencies with non-zero percentage of frequencies in the neighborhood of zero can give the algebraic tail to $n(\mathbf{r}_A, t)$. Parameter τ is linked therefore to the microscopic mechanism of capture, and parameter β is linked to the dynamics of the vibrating micromolecules.

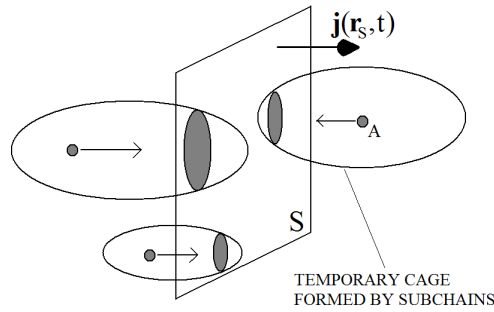


Figure 2. A virtual surface S cuts a collection of traps. The micromolecules, as they cross the surface, they collectively define an instantaneous flux \mathbf{j} .

Fractional equations with non-integer exponents in the time derivatives happen in anequilibrium phase transitions or whenever a dynamical system is trapped in some subspace of its state space of measure zero [9]. The time-related fractional exponent is linked to the waiting-time distribution of the walkers: $\Psi(\delta t)$. The distribution $\Psi(\delta t)$ is the pdf of the waiting times δt between two consecutive moves in a CTRW (Continuous Time Random Walk) approach. In such an approach subdiffusion happens when there is a wide distribution of waiting times [7]. In [9, 10] it is found that, for systems that are dynamically similar to ours,

$$\Psi(\delta t) \sim \delta t^{2/d_w - 1} \quad \text{for small } \delta t \quad (9)$$

The frequencies can be approached as $\nu \sim 1/\delta t$, and thus be linked to $\Psi(\delta t)$, where we see that we can have a frequency distribution with non-zero percentage of frequencies in the neighborhood of zero.

B. Construction and analysis of reduced A-molecule trajectories

Following Eyring's classical transition-state theory, the diffusion process is viewed, on the molecular scale (represented here by $\sigma_A, \sigma_B \cong 0.35$ nm), as a sequence of random molecular jumps of length λ [1]. Accordingly, successive positions \mathbf{r}_i ($i=1, 2, \dots, k$) separated by distances $\lambda=\sigma_A$ on the recorded A trajectories (thin lines in Fig. 3), were marked out as nodes of "reduced" A trajectories (bold lines in Fig. 3). A similar procedure has been recently followed in [11]. The latter trajectories were then checked for conformity to a random walk (RW), by evaluating the correlation coefficient $0 \leq S_{AA} \leq 1$:

$$S_{AA}(n) = \frac{1}{2} \left(3 \langle \cos^2 \theta_{AA}(m, m+n) \rangle - 1 \right) \quad (10)$$

where θ_{AA} represents the angle between the orientations of the m^{th} and $(m+n)^{\text{th}}$ step along a given reduced A trajectory and $S_{AA}(n)=0$ for a RW. The results (see Fig. 5), yield substantial $S_{AA}>0$ values, at least for $n=1$, which are significantly smaller in the case of FPE. This is good confirmatory evidence that the extent of observed deviation from ideal diffusion kinetics, illustrated in Fig. 1, reflects a degree and range of non-randomness of the relevant reduced diffusion trajectories, which can be quantified in terms of $S_{AA}(n)$.

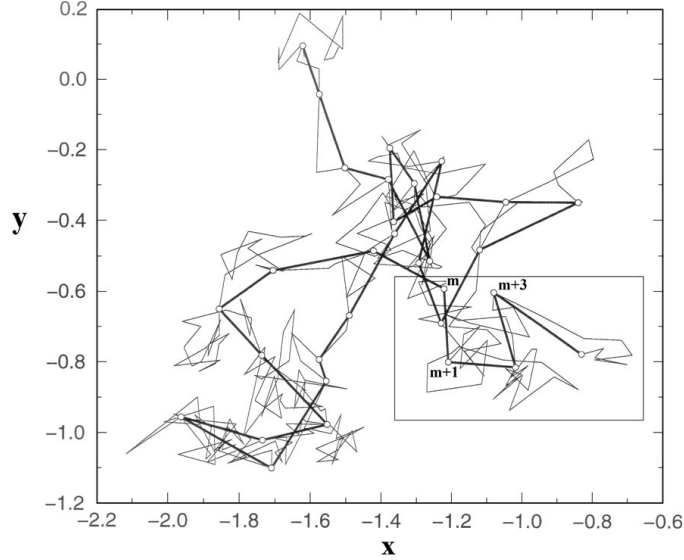


Figure 3. A 2-D projection of 3-D recorded and reduced diffusion trajectories.

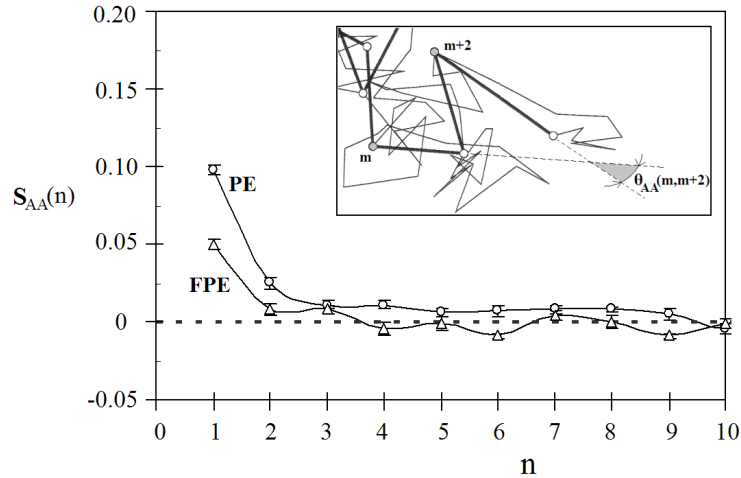


Figure 4. Test for deviation of diffusion trajectory from a random walk.

C. Detection and quantification of non-random amorphous polymer structure

We consider trimeric (-B-B-B-) subchains of PE or FPE and assign to them molecular orientation unit vectors \mathbf{u} defined by straight lines joining the end B's. We then characterize the degree and direction of “local preferred molecular orientation” (LPMO), at any given position \mathbf{r} in the polymer, in terms of the \mathbf{u} 's pertaining to “nearest-neighbor subchains (NNS)”, by defining a tensor (Fig. 5):

$$\mathbb{Q}(\mathbf{r}) = \langle \mathbf{u}\mathbf{u} \rangle_{\mathbf{r}} \quad (11)$$

(The NNS include trimers whose central B group lies within a sphere of suitable predetermined radius R_{\max} centered on \mathbf{r}). The lengths $L_1 > L_2 > L_3$ of the principal axes \mathbf{v}_i of the orientation ellipsoid, resulting from diagonalization of $\mathbb{Q}(\mathbf{r})$, yield the direction (\mathbf{v}_1) and magnitude (L_1) of the LPMO. The latter may be expressed as the *asphericity* $b = L_1^2 - 0.5(L_2^2 + L_3^2)$ which may vary from zero (random NNS orientations) to unity (parallel NNS). The probability distribution of b and resulting $\langle b \rangle$ offer a potentially useful way of characterizing linear polymers. Here, we find: $\langle b \rangle = 0.41$ (PE), 0.32 (FPE), implying that, as expected, higher chain flexibility induces increased NNS orientation randomness.

A tendency of the direction of LPMO to persist over significant distances signifies the presence of local anisotropic polymer structure, which is quantifiable via the correlation coefficient $0 \leq S_{BB} \leq 1$:

$$S_{BB}(n) = \frac{1}{2} \left(3 \langle \cos^2 \theta_{BB}(i, i+n) \rangle - 1 \right) \quad (12)$$

where θ_{BB} is the angle between the LPMO at the i^{th} and at the $(i+n)^{\text{th}}$ node in a real A-molecule reduced trajectory (open points in Fig. 6) or in a closely analogous random-walk of a virtual A molecule which probes primarily compact polymer sites (dark points in Fig. 6). The plots of Fig. 6 reveal substantial $S_{BB} > 0$ values detectable up to values of n exceeding 40 in the case of PE, which are considerably attenuated (but still quite significant) in the case of FPE. The latter fact, in conjunction with the similarity of real and virtual-A S_{BB} plots, confirms the presence of inherent (rather than penetrant-induced) polymer nanostructure.

D. Relation between nanostructure and local diffusion path

Computation of a correlation coefficient $0 \leq S_{AB} \leq 1$, defined a

$$S_{AB} = \frac{1}{2} \left(3 \langle \cos^2 \theta_{AB}(j, j+1) \rangle - 1 \right) \quad (13)$$

where θ_{AB} is the angle between a diffusion step linking nodes $j, j+1$ of a real reduced A trajectory and the mean LPMO between these nodes, gave $S_{AB} \approx 0.10$ (PE), 0.06 (FPE), well above $S_{AB} = 0$ for a random walk. These results demonstrate a clear tendency of the local motion of diffusing molecules to follow a preferred direction in line with that of persisting LPMO in the surrounding polymer. This tendency is clearly weaker in FPE, in line with its less prominent nanostructure (Fig. 6) and the smaller deviation of diffusion therein from a random walk (Fig. 4).

In Fig. 7, S_{AB} is shown for several λ values. In PE a significant correlation is detected, the range of which indicates that it is intimately related to anomalous diffusion. In FPE we also see a correlation, of somewhat diminished intensity but of comparable extent. This picture is compatible with the presence of elongated cavities temporarily trapping the micromolecule. The decrease of S_{AB} for small λ happens because there the RT mostly samples the more or less random rattling. The decrease of S_{AB} for large λ happens because there the RT mostly samples jumps of the micromolecule between uncorrelated cavities. The length scale where S_{AB} is strong is compatible to the extent of the anomalous diffusion. We may therefore confidently attribute the observed deviation from ideal diffusion kinetics (Fig. 1) to the presence of anisotropic nanostructure in the amorphous polymer.

III. MOL_DYGEST

The presented analyses were performed using `mol_dygest` – a software package for the dynamic and geometric study of molecular trajectories. This is a software system, build by one of the authors (C. S. C.), which can perform a detailed geometry-dynamics trajectory analysis on the output of a MD program. `mol_dygest` (a) is able to analyze very large input files on a limited-main-memory

computer, (b) is able to perform flexibly all requested analyses by small run-time programs with adjustability on the output detail, (c) includes a simple programming language named `mdl`, `mol_dygest_language`, that orchestrates all analyses and greatly augments the user-friendliness of the system. An excerpt of a program written in `mdl` is:

```

directives:
  calculate_ = reduced_trajec ( use_lamda = 0.29, set_fractal = OFF )
  calculate_ = set_up ( use_b_nei_radius = 0.38 , set_red_traj = ON )
  calculate_ = sab ( use_sdiv = 10 )
end.

```

A full program in `mdl` resides in two different files. In the first file, named `mol_dygest_defin`, the definitions and physical units of the MD program that produces the trajectories are declared, and in the second file, named `mol_dygest_direc`, the analysis directives are given. Normally the contents of the first file are very rarely altered. The second file, in contrast, is expected to change frequently, depending on what analyses the user wishes to perform. The compiler of `mdl`, called `mol_dygest_driv`, educated by the information and directives that reside in the two files, builds the Fortran source, called `mol_dygest_runT`, which actually performs all analyses requested. While building `mol_dygest_runT` the `mol_dygest_driv` seeks and uses code from `mol_dygest_lib` collection of parameterized routines. The run-time program `mol_dygest_runT` is optimized for speed and memory management and the resulted Fortran 77 code is portable. The driver, `mol_dygest_driv`, itself is also coded in readable and portable Fortran 77 (it has run from UNIX-based Convex mainframes, to Wintel PCs.).

`mol_dygest_driv` is a compiler with extensive error reporting capabilities that performs lexical and semantic analysis on its two input files before embarking on generating `mol_dygest_runT`, informing the user of possible syntactic errors or inconsistencies on the requested analyses. The available geometric - dynamic analyses possible in the current realization of `mdl` are activated using the `calculate_` keyword respecting the syntactic rule:

```

calculate_ = <calc_ident> ( [(<keyw>_<param>=<value>) {(,|; eol) (<keyw>_<param>=<value>)}] )

```

Depending on what `<calc_ident>` is, several `<param>`, `<value>` pairs are available. Some analysis directives are briefly described in table 1. The `mol_dygest` package is available from C. S. C.

<code><calc_ident></code>	Description
<code>reduced_trajec</code>	<i>Calculation of the reduced trajectory.</i>
<code>saa</code>	<i>Analysis based on eq. (10) along the reduced trajectory currently defined.</i>
<code>sbb</code>	<i>Analysis of the persistence of the LPMO based on eqs. (11) and (12).</i>
<code>sab</code>	<i>Analysis based on eq. (13) of the interplay of LPMO and micromolecular displacement.</i>

Table 1: Some `mol_dygest` analysis directives.

IV. REFERENCES

- [1] C. S. Chassapis, J. K. Petrou, J. H. Petropoulos, D. N. Theodorou, *Macromolecules*, Vol 29 (1996) 3615-3624.
- [2] H. Takeuchi, K. Okazaki, *J. Chem. Phys.*, Vol. 92 (1990) 5643-5652.
- [3] R.-J. Roe, *Journal of non-crystalline solids*, Vols 172-174 (1994) 77-87.
- [4] G. D. Smith, D. Y. Yoon, R. L. Jaffe, *Macromolecules*, Vol 28 (1995) 5897-5905.

- [5] J.-F. Gouyet, "Diffusion in heterogeneous materials". In A.L. Laskar et al. (eds.), *Diffusion in Materials*, Kluger Academic Publishers, The Netherlands, 1990.
- [6] S. Havlin, D. Ben-Avraham, *Advances in Physics*, Vol 36 (1987) 695-798.
- [7] M. B. Isichenko, *Reviews of Modern Physics*, Vol 64 (1992) 961-1043.
- [8] R. Metzler, W. G. Glöckle, T. F. Nonnenmacher, *Physica A*, Vol 211 (1994) 13-24.
- [9] R. Hilfer, L. Anton, *Physical Review E*, Vol 51 (1995) R848-R851.
- [10] W. G. Glöckle, T. F. Nonnenmacher, *Journal of Statistical Physics*, Vol 71 (1993) 741-757.
- [11] G. E. Karlsson, U. W. Gedde and M. S. Hedenqvist, *Polymer*, Vol 45 (2004) 3893-3900.

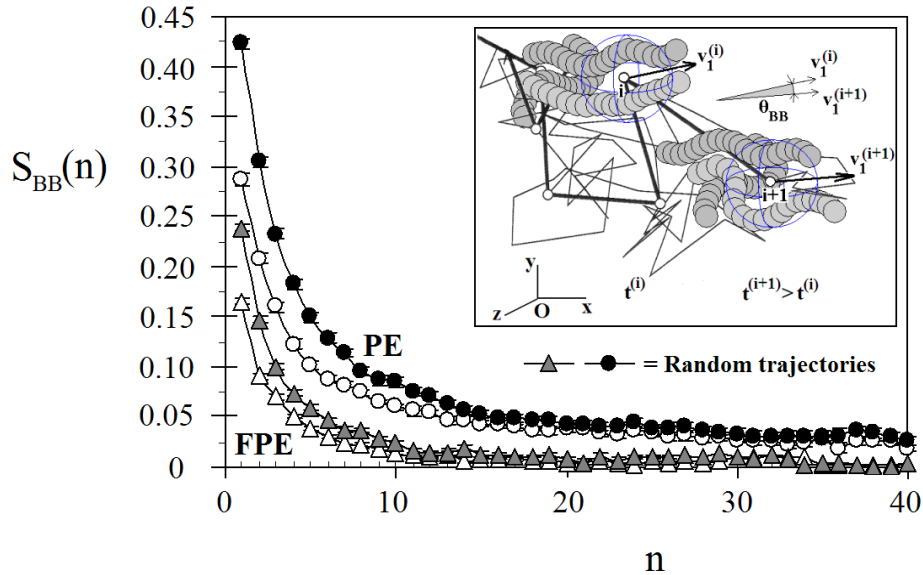


Figure 6. Test for non-random polymer structure.

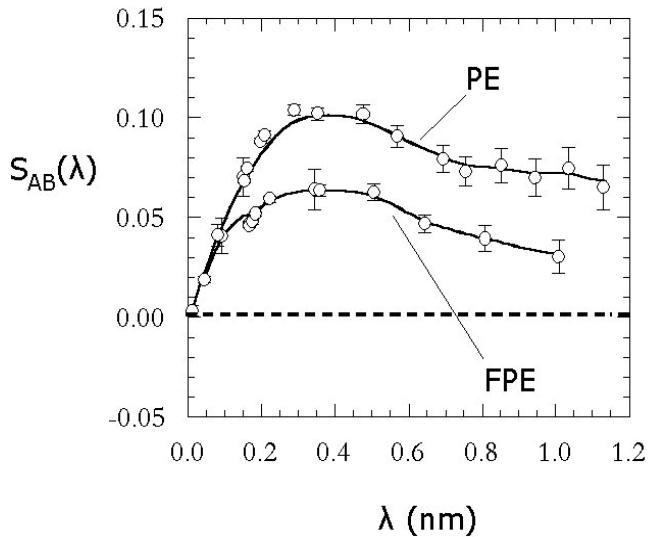


Figure 7. Clear display of the interplay between LPMO and the movement of the micromolecules, for several molecular scales

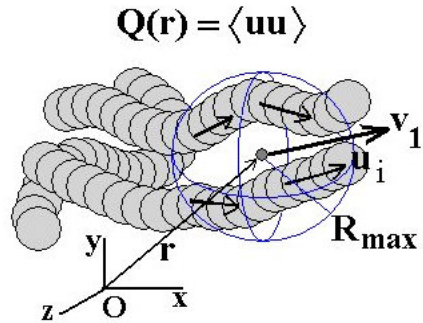


Figure 5. Defining the tensor $Q(r)$.